

A critical analysis of the modelling of dissipation in fission^{*}

B. Jurado^{1†}, K.-H. Schmidt¹, J. Benlliure², A. R. Junghans³

¹*GSI, Planckstr.1, 64291 Darmstadt, Germany*

²*University of Santiago de Compostela, 15706 Santiago de Compostela, Spain*

³*University of Washington, CENPA, Box 354290, Seattle WA 98195, USA*

Abstract: We examine the modelling of the effects of dissipation in fission by analysing experimental data where fission is induced by peripheral heavy-ion collisions at relativistic energies. Our results are based on the analysis of available data of the total nuclear fission cross sections of ^{238}U at $1\text{-}A$ GeV on Au and U targets with an abrasion-evaporation code that contains an intermediate break-up stage. We have incorporated in the code three different approximations for the time-dependent fission-decay width that describe the hindrance of fission due to dissipation. One is a highly realistic description based on the analytical solution of the Fokker-Planck equation when the nuclear potential is approximated by a parabola. The two others correspond to the most widely used approximations, a step function and an exponential-like in-growth function. The experimental data are only reproduced when dissipation effects are considered. However, the deduced value of the reduced dissipation coefficient β depends strongly on the approximation applied. A careful analysis sheds severe doubts on the use of the exponential-like in-growth function for describing the time dependence of the fission width.

PACS: 24.10.-i; 24.75.+i; 25.75.-q

Keywords: Nuclear fission; dissipation effects; time-dependent fission-decay width; Fokker-Planck equation; analytical approximation

1.Introduction

In their transition-state model [1], Bohr and Wheeler described the fission process of an excited heavy nucleus according to a purely statistical point of view. Soon after, Kramers [2] suggested describing fission as a diffusion process where the evolution of the fission degree of freedom by spreading into the deformation space is determined by dissipation, that is, by the interaction of the fission collective degree of freedom with the heat bath formed by the individual nucleons. Such process can be described by the Fokker-Planck equation [3] (FPE). In this specific case, the variable of the FPE is the time-dependent probability distribution $W(x,p,t)$ as a function of the deformation in fission direction x and its canonically conjugate momentum p . Kramers found that the stationary solution of the FPE leads to a reduction of the fission width compared to the fission width predicted by the transition-state model of Bohr and Wheeler by a factor

$$K = \left[1 + \left(\frac{\beta}{2\omega_0} \right)^2 \right]^{1/2} - \frac{\beta}{2\omega_0} \quad (1)$$

where β is the reduced dissipation coefficient, which appears as a parameter in the Fokker-Planck equation, and ω_0 is the frequency of the harmonic-oscillator potential that osculates the fission barrier at the saddle point. However, the success of the transition-state model prevented this idea of Kramers to establish. Approximately forty years later, experimentally observed high pre-scission neutron multiplicities [4,5] gave the impetus to Grangé, Jun-Qing and Weidenmüller [6] and others to theoretically investigate the influence of nuclear

^{*} This work forms part of the PhD thesis of B. Jurado

[†] Corresponding author: B. Jurado, GANIL, Boulevard Henry Becquerel, B.P. 5027, 14076 Caen CEDEX 5, France, e-mail: jurado@ganil.fr (present address)

dissipation on the fission time scale. They solved the time-dependent FPE numerically, starting from a spherical or a nearly spherical shape. Under such conditions, the solution of the FPE leads to a time-dependent fission width $\Gamma_f(t)$ that is first suppressed, then increases and finally reaches the asymptotic value given by the Kramers fission width. The time evolution of the fission width is characterised by the transient time τ_f defined as the time in which $\Gamma_f(t)$ reaches 90% of the asymptotic value [7]. The dependence of the transient time from the reduced dissipation coefficient β can be deduced by solving the FPE. In reference [7] the following approximate relations were established:

$$\begin{aligned}\tau_f &= \frac{1}{\beta} \ln\left(\frac{10B_f}{T}\right) & \text{for } \beta < 2\omega_x \\ \tau_f &= \frac{\beta}{2\omega_x^2} \ln\left(\frac{10B_f}{T}\right) & \text{for } \beta \geq 2\omega_x\end{aligned}\tag{2}$$

where B_f is the fission barrier, T is the nuclear temperature and ω_x is an effective oscillator frequency* at the ground state.

The magnitude of the reduced dissipation coefficient β remained a subject of intense investigations, both theoretically and experimentally. Theoretical efforts to predict nuclear dissipation rely on e.g. the one-body dissipation mechanism [8], the decay of diabatic [9] excitations, and the linear-response theory [10]. Experimental efforts to determine nuclear dissipation rely on the analysis of pre- and post-scission neutron multiplicities [11, 12], of the strength of the decay of the giant dipole resonance [13] in highly excited nuclei, of charged-particle multiplicities [14, 15], of evaporation-residue cross sections [16, 17] and fission cross sections [18], and on direct measurements of the fission lifetimes [19]. In spite of these efforts, the value of the reduced dissipation coefficient [20] and more exactly its variation with deformation and temperature is still subject of debate. In reference [21] the analysis of pre-scission giant dipole resonance γ -rays pointed to an onset of dissipation at excitation energies around 40 to 60 MeV. Later in reference [22], the study of the pre-scission neutron multiplicities of a set of fast-fission reactions lead to a strong dependence of dissipation on temperature as well. However, several works [23, 24] have already remarked the difficulty of finding experimental signatures sensitive to the temperature dependence of dissipation. On the other hand, according to recent experimental results, a rather consistent picture on the deformation dependence of dissipation seems to emerge. Strong dissipative effects have been observed within the large-deformation regime from the saddle point to scission [12, 25, 26, 27], while in the small-deformation regime from the ground state to the saddle point the effects of dissipation are rather weaker. However, in the small-deformation regime, on which we concentrate in the present work, the magnitude of the dissipation effects is rather uncertain. Some works point to clear effects [24, 28], whereas others point to quite weak or no dissipation effects [16, 17, 29, 30].

From the experimental side, the difficulty of the problem has several reasons. Transient effects on the fission-decay rate can only be deduced under certain conditions. Since transient effects are related to the process of equilibrating the distribution in deformation space and in the conjugate momentum, the corresponding initial distributions, populated by the nuclear-reaction mechanism, must be well defined and significantly differ from equilibrium. Most of

* According to [7], ω_x is the effective harmonic oscillator frequency around the ground state for the true nuclear potential (see full line in figure 1a). It deviates slightly from the frequency ω_l of the harmonic approximation (see dashed line figure 1a). In literature, expression (2) is mostly used approximating ω_x by ω_l .

the experiments dedicated to the investigation of dissipation are based on heavy-ion induced fusion-fission, fast-fission and quasi-fission reactions, which do not offer optimum conditions for extracting the signatures of dissipation at small deformation. These reactions cannot be analysed with the model of reference [6] because the initial conditions of the composite system formed after the collision do not correspond to those assumed in [6]. Such reactions require elaborate dynamical models that have to take into account fluctuations with respect to the mean dynamical trajectory and the large angular momentum of the composite system formed in the reaction. Incidentally, a considerable effort has been made lately in the development of dynamical codes; for instance a recent formulation of such description based on the Langevin equation is presented in reference [31], and in reference [32] it is investigated whether the statistical evaporation model is applicable for particle emission along quasifission trajectories. In addition, the reaction mechanism should be chosen in a way that transient effects modify the fission-decay rate in a noticeable way, which, in the asymptotic case, follows an exponential time distribution with a decay constant given by the total decay width. This is the case only if the excitation energy of the nucleus is high enough for the statistical decay time to be shorter than the transient time. Thus, an experimental approach is required that produces highly excited heavy nuclei with high cross sections.

Provided the initial conditions of the excited nucleus fulfil the requirements of the model of reference [6], investigating the effects of dissipation in the deexcitation process of such nucleus implies modelling the time-dependent onset of the flux over the fission barrier that is expressed by a time-dependent fission decay width $\Gamma_f(t)$. This is a rather difficult task, and most of the model calculations contain one of the following approximations for $\Gamma_f(t)$:

- A step function that sets in at time τ_f :
$$\Gamma_f(t) = \begin{cases} 0, & t < \tau_f \\ \Gamma_f^k, & t \geq \tau_f \end{cases} \quad (3)$$

- An exponential in-growth function:
$$\Gamma_f(t) = \Gamma_f^k \cdot \{1 - \exp(-t/\tau)\} \quad (4)$$

where $\tau = \tau_f/2.3$, τ_f is the transient time and Γ_f^k is the Bohr-Wheeler [1] fission width, multiplied by the Kramers factor K of equation (1). The questions, how well each of the approximations does reproduce the behaviour of $\Gamma_f(t)$ that results from solving the FPE, how accurate is their implementation in the theoretical codes and how the approximations influence the final result have not been properly analysed yet.

In the present work, we make several efforts to solve these problems. Firstly, we chose an experimental approach that most closely corresponds to the conditions under which Grangé, Jun-Qing and Weidenmüller formulated their model. Secondly, we apply a highly realistic description of the in-growth function governing the onset of the fission process. This function is obtained by using the analytical solution of the FPE for a parabolic nuclear potential. Additionally, in the implementation of the in-growth functions given by equations (3) and (4) in the nuclear-reaction code we remove some unnecessary approximations that were used in previous formulations. Finally, we investigate to which degree the value of the dissipation coefficient deduced from experimental data depends on the shape of the in-growth function used in the analysis. Our results shed severe doubts on several conclusions drawn in previous work. These questions have already been briefly assessed in reference [33].

2. Experimental approach

It is our aim to base our analysis on an experimental approach that meets the conditions of the theoretical work of reference [6] as closely as possible. That means, a nucleus should be highly excited with only little shape distortion. In addition, the angular momentum [34] induced should be small in order to avoid additional influence on the fission process. This aim can be achieved by applying a projectile-fragmentation reaction, i.e. a very peripheral nuclear collision with relativistic heavy ions. Compared to previous quite interesting attempts to reach this goal by relativistic proton-nucleus collisions in inverse kinematics [28] and the annihilation of antiprotons [35, 36] at the nuclear surface, this approach populates higher excitation energies more strongly, up to the onset of multifragmentation [37].

If the excitation energy of the nucleus is higher than the limiting excitation energy at which the statistical-decay time and the transient time τ_f become comparable, fission competition is delayed with respect to particle evaporation by the transient time. During the transient time, the emission of particles leads to a decrease of the excitation energy. Therefore, in reactions that induce excitation energies above the limiting value, the existence of a transient time would imply a considerable reduction of the fission probability (and hence of the fission cross section) compared to the predictions of the transition-state model.

In this work, we analyse the total nuclear fission cross sections of ^{238}U at 1.4 GeV on gold and uranium targets. The nuclear fission cross sections have been determined by Rubehn et al. [38] subtracting the electromagnetic contribution from the experimental total fission cross sections of ^{238}U (1.4 GeV) on gold and uranium measured in the same reference [38]. The values of the cross sections are listed in table 1.

3. Discussion

3.1 Total nuclear fission cross sections

The experimental data of table 1 are compared with several calculations performed with an extended version of the abrasion-ablation Monte-Carlo code ABRABLA [39, 40]. This code consists of three stages. In the first stage the properties of the nucleus after the fragmentation reaction are calculated according to the abrasion model. As was determined experimentally in reference [41], an average excitation energy of 27 MeV per nucleon abraded is induced. This value is in agreement with predictions for peripheral collisions based on BUU calculations [42]. The angular momentum deduced is estimated according to reference [34]. The second stage accounts for the simultaneous emission of nucleons and clusters (simultaneous break-up) that takes place due to thermal instabilities when the temperature of the projectile spectator exceeds 5.5 MeV [43]; this part is described further below. The simultaneous emission makes the nucleus cool down to a temperature of 5.5 MeV. The break-up stage is assumed to be very fast, and thus the fission collective degree of freedom is not excited. From this moment on the third stage, the sequential decay, sets in, which is described by the statistical model. It treats the deexcitation of the nucleus by particle evaporation and fission. This last part has been modified to account for dissipation effects incorporating three different descriptions of $\Gamma_f(t)$. We included the approximations given by equations (3) and (4) of section 1 avoiding several further approximations applied in previous formulations [13, 44, 45, 46]. In addition, we integrated a highly realistic description of $\Gamma_f(t)$ based on the analytical solution of the FPE when the deformation dependence of the nuclear potential between the ground state and the saddle point is approximated by a parabola; this function is thoroughly discussed further below. A detailed description on how these three functions have been

implemented can be found in the appendix. Besides the treatment of the dissipation effects, the ratio of the level-density parameters a_f/a_n and the fission barriers B_f are the most critical ingredients of the model. The deformation dependence of the level-density parameter has been discussed in references [47, 48, 49]. In our case, the ratio a_f/a_n is calculated considering volume and surface dependencies as proposed in reference [49] according to the expression:

$$a = \alpha_v A + \alpha_s A^{2/3} B_s + \alpha_k A^{1/3} B_k \quad (5)$$

where α_v , α_s and α_k are the coefficients of the volume, surface and curvature components of the single-particle level densities, respectively, with the values $\alpha_v = 0.073 \text{ MeV}^{-1}$, $\alpha_s = 0.095 \text{ MeV}^{-1}$ and $\alpha_k = 0 \text{ MeV}^{-1}$. B_s and B_k are the ratios of the surface of the deformed nucleus and the integrated curvature of the nucleus, respectively, related to the corresponding values of a spherical nucleus. Their values are taken from reference [50]. The angular-momentum-dependent fission barriers are taken from the finite-range liquid-drop model predictions of Sierk [51]. As demonstrated in reference [28], a recent experimental determination of these parameters by K. X. Jing and co-workers [52], based on the measurement of cumulative fission probabilities of neighbouring isotopes, is in very good agreement with these theoretical predictions.

	σ_f^{nucl} on Au /b		σ_f^{nucl} on U /b	
Experimental Data	2.14 ± 0.22		2.19 ± 0.44	
Calculation	No break-up	Break-up	No Break-up	Break-up
Transition-State Model	5.53	3.28	5.80	3.39
$\Gamma_f(t)$ step $\beta = 2 \cdot 10^{21} \text{ s}^{-1}$	2.15	2.04	2.20	2.03
$\Gamma_f(t)$ step $\beta = 4 \cdot 10^{21} \text{ s}^{-1}$	1.58	1.50	1.59	1.56
$\Gamma_f(t) \sim 1 - \exp(-t/\tau)$ $\beta = 2 \cdot 10^{21} \text{ s}^{-1}$	4.92	2.52	5.16	2.61
$\Gamma_f(t) \sim 1 - \exp(-t/\tau)$ $\beta = 4 \cdot 10^{21} \text{ s}^{-1}$	4.31	2.02	4.50	2.06
$\Gamma_f(t)$ FPE $\beta = 2 \cdot 10^{21} \text{ s}^{-1}$	2.28	2.08	2.39	2.13

Table 1: Experimental total nuclear fission cross sections of $^{238}\text{U}(1.4 \text{ GeV})$ on gold and uranium targets compared with different calculations performed with the code ABRABLA. The experimental cross sections are taken from [38]. Each calculation has been performed twice. In one case, the simultaneous break-up stage is not included in the calculation, so that no limit for the initial temperature of the sequential decay (evaporation cascade) is imposed. In the other case, the break-up model imposes an upper limit of 5.5 MeV to the initial temperature of the evaporation cascade. A first set of calculations was performed with the transition-state model [1]. The other calculations were performed with different descriptions of $\Gamma_f(t)$ and different values of β . The last calculation was performed with $\Gamma_f(t)$ as the analytical solution of the FPE given by equation (20) with $W^{\text{par}}(x=x_b, t)$ taken from equations (7) and (8).

The calculations presented in table 1 were performed with different options. Different shapes of the time-dependent fission width and different values of β were used. In addition, for part of the calculations the break-up stage of the code was not included. Though this is unphysical, it serves to distinguish between the effects of dissipation and the effects of the break-up process on fission at high excitation energies. For the moment, we will consider the calculations performed including break-up to describe the intermediate stage between the abrasion and the statistical evaporation at temperatures larger than 5.5 MeV. As the values of the fourth row of table 1 show, the transition-state model [1] clearly overestimates the experimental data. In fact, the experimental cross sections are only reproduced when dissipative effects are included in the calculation. However, the choice of the in-growth function for $\Gamma_f(t)$ according to equations (3) or (4) has a strong influence on the dissipation coefficient deduced. While the calculation with the description given by equation (3) (step function) reproduces the data with a value of $\beta = 2 \cdot 10^{21} \text{ s}^{-1}$, the same value of β with equation (4) (exponential like in-growth) overestimates the cross sections. The reason is that in the latter case fission is already possible with a considerable probability at the very beginning of the deexcitation process. To reproduce the data when the exponential-like in-growth function is used, a larger value of the dissipation coefficient $\beta = 4 \cdot 10^{21} \text{ s}^{-1}$ is required that reduces the asymptotic value of the fission width and enlarges the transient time. As expected, when this value of β is used with the step function, the cross sections are underestimated.

3.2 Critical view on the exponential approximation for the fission decay width

Although the measured fission cross sections can be described by the exponential-like in-growth function, equation (4), by adjusting the dissipation coefficient, this representation does not reproduce the behaviour of $\Gamma_f(t)$ predicted by the FPE. This will become clear after the following considerations. In reference [6], the time-dependent fission width is defined as

$$\Gamma_f(t) = \hbar \lambda_f = \hbar \frac{\int_{-\infty}^{+\infty} v W(x = x_b, v, t) dv}{\int_{-\infty}^{+\infty} \int_{-\infty}^{+\infty} W(x, v, t) dv dx} \quad (6)$$

Here λ_f is the fission rate, x_b is the deformation at the barrier, v is the velocity ($v = \frac{\partial x}{\partial t}$) and W is the probability distribution. The denominator measures the part of the probability distribution still caught inside the fission barrier. Due to the flux over the fission barrier, the value of the denominator gradually decreases.

According to the initial conditions assumed, at the beginning of the sequential deexcitation process, the probability distribution can be represented by a narrow Gaussian centred at the ground-state deformation. As was already discussed by Grangé and Weidenmüller, part of the intrinsic excitation energy is transferred to the fission collective degree of freedom. After a certain time that depends on the value of β , the collective energy saturates, and the probability distribution gradually broadens in deformation space, eventually reaching the fission-barrier deformation x_b . We explicitly investigate the time evolution of the probability $W(x=x_b, t)$ at the barrier deformation x_b in figure 1. First, we evaluate the probability distribution $W(x=x_b, t)$ at the deformation x_b as a function of time by solving the FPE [53] when the nuclear potential is approximated by the parabola represented by the dashed line on figure 1a). The deformation x_b is defined as well in figure 1a). The solution of $W(x=x_b, t)$ is shown by the dashed line in figure 1b). Although this solution of the FPE is obtained for the parabolic potential, the total suppression of the probability distribution at the fission barrier for the initial part of the deexcitation process also results for a more realistic potential. In fact, this

feature is independent of the shape of the nuclear potential. This is confirmed by the dotted line of figure 1b) that depicts the solution of the FPE for $W(x=x_b, t)$ with the very shallow parabolic potential represented by the dotted curve in figure 1a). One might have expected that a flat potential would lead to an instantaneous spread of the probability distribution up to the saddle deformation. However, the dotted line of figure 1b) shows that the probability distribution at x_b starts differing from zero only after some time. Indeed, the probability $W(x=x_b, t)$ remains essentially zero up to $t \approx 0.6 \cdot 10^{-21}$ s in both cases, for the shallow and for the deep parabola.

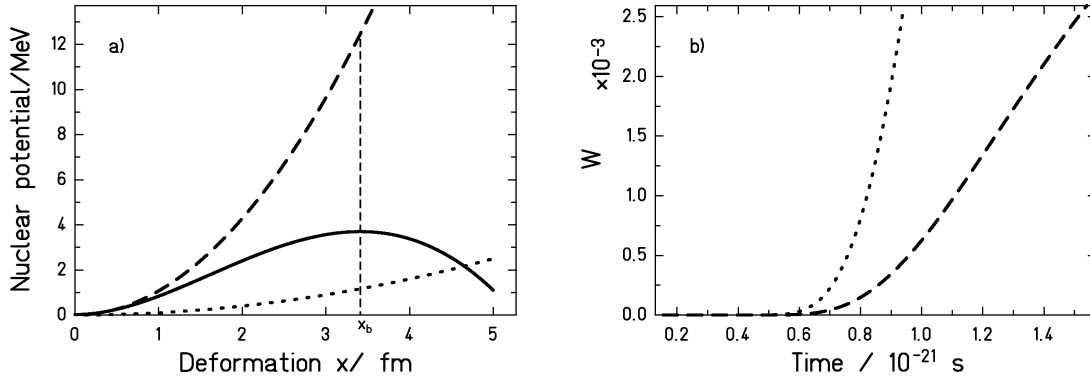


Figure 1: a) Nuclear potential as a function of deformation, the minimum at zero deformation corresponds to the ground state. The full line represents the nuclear potential chosen in reference [7] ($U = 8.61 \cdot 10^{-3}(x-3.41)^2 \cdot [(x-23.098)(x-1.59)] + 3.7$) for a nucleus with mass $A = 248$. Using the reduced mass $A/4$ [7] leads to the ground-state frequency $\omega_I = 1.83 \cdot 10^{21} \text{s}^{-1}$ in the harmonic approximation, and the maximum reproduces the fission barrier at deformation x_b with a frequency $\omega_o = 1.65 \cdot 10^{21} \text{s}^{-1}$. The dashed line is a parabola with the same ground-state frequency $\omega_I = 1.83 \cdot 10^{21} \text{s}^{-1}$, and the dotted line is a parabola with the strongly reduced ground-state frequency $\omega_I = 0.55 \cdot 10^{21} \text{s}^{-1}$ for the same nucleus.

b) Probability $W(x = x_b, t) = \int_{-\infty}^{+\infty} W(x = x_b, v, t) dv$ evaluated at the deformation x_b as a function of time for the two parabolic potentials plotted on the left. The other parameters used in both calculations are also chosen as in reference [7], i.e., $\beta = 5 \cdot 10^{21} \text{s}^{-1}$, $T = 3 \text{ MeV}$, $A = 248$ and reduced mass $A/4$. The dashed line is the solution of the FPE when the nuclear potential is approximated by the dashed line on figure 1a). The dotted line is the solution of the FPE when using the potential represented by the dotted line on figure 1a).

According to equation (6), the fission width will vanish when the probability $W(x=x_b, t)$ vanishes. Hence, independently of the nuclear potential, $\Gamma_f(t)$ should be zero and have a zero slope at the initial time. This can be observed as well in figure 2a), where the numerical solution of the FPE obtained in reference [7] for the fission rate $\lambda_f(t) = \Gamma_f(t)/\hbar$ is compared with the exponential in-growth function and the step function. This picture shows that the exponential function starts with a very steep slope contradicting the previous requirement of complete suppression at the initial time. On the other hand, the step function reproduces the hindrance of fission at the beginning of the process but it overestimates its duration. In our opinion, this fact could be improved by opening the fission channel by the step function at the time in which the fission probability of the exact solution has reached around 50% of its

stationary value or even less, instead of the standard value of 90%, introduced in ref [7]. Indeed, we will see later that the onset of the fission width is of particular importance.

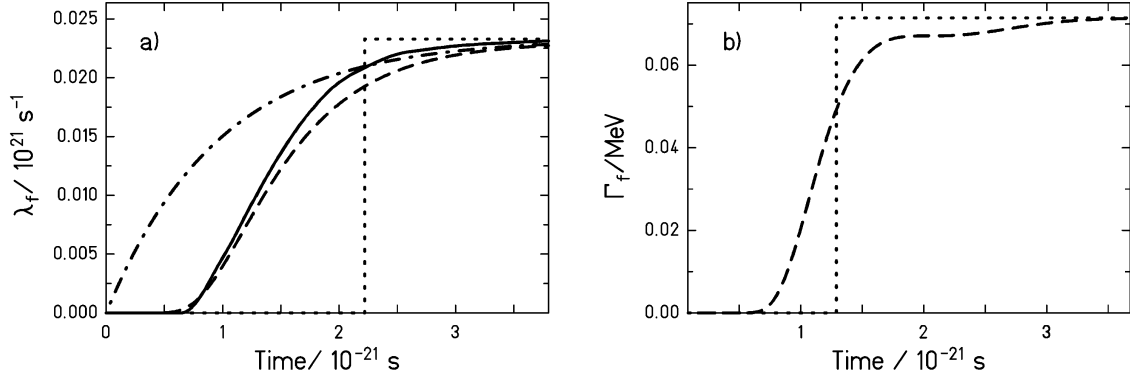


Figure 2: a) Fission rate $\lambda_f(t) = \Gamma_f(t)/\hbar$ as a function of time for $\beta = 5 \cdot 10^{21} \text{ s}^{-1}$, $T = 3 \text{ MeV}$ and $A = 248$. The full line is the numerical solution of the FPE taken from reference [7]. The nuclear potential used in this calculation is represented by the full line in figure 1a). The dashed line is calculated using equation (20) with $W(x=x_b, t)$ taken from equations (7) and (8). The dotted line corresponds to $\lambda_f(t)$ given by the step function according to equation (3), and the dashed-dotted line corresponds to $\lambda_f(t)$ given by the exponential-like function described by equation (4), both calculated with parameters leading to the same transient time as the full calculation. b) Fission width as a function of time for $\beta = 2 \cdot 10^{21} \text{ s}^{-1}$; the rest of the parameters are as in part a). The dashed line is calculated using equation (20) with $W^{\text{par}}(x = x_b, t)$ taken from equations (7) and (8). The dotted line corresponds to $\Gamma_f(t)$ given by equation (3).

It is worthwhile to have a closer look on the case of a parabolic potential, where an analytic solution of the Fokker-Planck equation is available. The solution of the Fokker-Planck equation for $W(x = x_b, t)$ with a nuclear potential approximated by a parabola [53], assuming zero deformation and zero velocity as initial conditions, is given by the function

$$W^{\text{par}}(x = x_b, t) = \frac{1}{\sqrt{2\pi\sigma}} \cdot \exp\left(-\frac{x_b^2}{2\sigma^2}\right) \quad (7)$$

where σ^2 is a time-dependent function of the form:

$$\sigma^2 = \frac{kT}{\mu\omega_1^2} \left\{ 1 - \exp(-\beta \cdot t) \cdot \left[\frac{2\beta^2}{\beta_1^2} \sinh^2\left(\frac{1}{2}\beta_1 t\right) + \frac{\beta}{\beta_1} \sinh(\beta_1 t) + 1 \right] \right\} \quad (8)$$

where k is Boltzmann's constant, T is the nuclear temperature, μ is the reduced mass associated to the deformation degree of freedom, ω_1 describes the curvature of the potential at the ground state and $\beta_1 = (\beta^2 - 4\omega_1^2)^{1/2}$. The physical meaning of function (8) can be better understood when we consider large times and β in the overdamped regime ($\beta \gg 2\omega_1$). Under these conditions, we can neglect the terms $\exp(-\beta_1 t)$, and β_1 can be approximated by $\beta_1 \approx \beta - 2\omega_1^2/\beta$. With this, expression (8) turns to:

$$\sigma^2 \approx \frac{kT}{\mu\omega_1^2} \left\{ 1 - \frac{1}{2} \left[\frac{\beta^2}{\beta_1^2} + \frac{\beta}{\beta_1} \right] \cdot \exp\left(-\frac{2\omega_1^2}{\beta} \cdot t\right) \right\} \quad (9)$$

whereby the negative values at small times should be replaced by zero. Using the further approximation $\beta_l \approx \beta$ in the preexponential factor, we obtain

$$\sigma^2 \approx \frac{kT}{\mu\omega_1^2} \left\{ 1 - \exp\left(-\frac{2\omega_1^2}{\beta} \cdot t\right) \right\} \quad (10)$$

Actually, equation (10) is already quantitatively very similar to (8) for $\beta \geq 5 \cdot 10^{21} \text{ s}^{-1}$. Equation (10) shows that the process of the population of the deformation space can be described by a probability distribution with the shape of a Gaussian whose second moment exponentially approaches the asymptotic value. This fact might have misled some authors to introduce an exponential-like in-growth function to picture the variation of the fission width with time. We would like to stress here that it is the second moment of the probability distribution that approximately grows like $1 - \exp(-t/\tau)$ and not the fission width itself.

3.3 New analytical approximation for the time-dependent fission decay width

In the overdamped regime, $W(x, v, t)$ is equilibrated in velocity very fast. Under these conditions, the FPE transforms into the Smoluchowski equation [3].

$$\frac{\partial}{\partial t} W(x, t) = \beta^{-1} \frac{\partial}{\partial x} \left[\mu^{-1} \frac{dU}{dx} W(x, t) \right] + \varepsilon \beta^{-2} \frac{\partial^2}{\partial x^2} W(x, t) \quad (11)$$

where μ is the reduced mass, $U(x)$ is the nuclear potential and $\varepsilon = \beta kT/\mu$. An analytical approximate solution to this equation for a realistic potential, valid for $t > \beta/2 \omega_1^2$, is presented in reference [7]. However, for short times, where the dissipation has a decisive effect on the deexcitation process, this solution does not fulfil the requirement to vanish for a certain time. For this reason, we propose the following more appropriate alternative to this formulation.

In the following, the various steps to derive a very realistic approximation for the fission-decay width will be illustrated in detail. A short description has already been presented in reference [33]. First of all we will develop a slightly modified expression for the exact description of the fission-decay width, whose definition is given by equation (6). We start by defining the normalised probability distribution $W_n(x = x_b, v, t)$ at the fission-barrier deformation x_b as:

$$W_n(x = x_b, v, t) = \frac{W(x = x_b, v, t)}{\int_{-\infty-\infty}^{x_b+\infty} \int W(x, v, t) dv dx} \quad (12)$$

Considering equation (12), the fission width of equation (6), can be reformulated as follows:

$$\Gamma_f(t) = \hbar \int_{-\infty}^{+\infty} v W_n(x = x_b, v, t) dv \quad (13)$$

In the stationary case we get:

$$\Gamma_f(t \rightarrow \infty) = \hbar \int_{-\infty}^{+\infty} v W_n(x = x_b, v, t \rightarrow \infty) dv = \Gamma_f^K \quad (14)$$

The value of Γ_f^K has already been derived by Kramers [2].

Finally, combining equations (13) and (14) we can reformulate the time-dependent fission width defined by equation (6) as:

$$\Gamma_f(t) = \frac{\int_{-\infty}^{+\infty} v W_n(x = x_b, v, t) dv}{\int_{-\infty}^{+\infty} v W_n(x = x_b, v, t \rightarrow \infty) dv} \Gamma_f^K \quad (15)$$

At this point we introduce the two approximations that lead to a new description of the time-dependent fission width. The first approximation is to consider that:

$$W_n(x = x_b, v, t) \approx C(t) \cdot W_n(x = x_b, v, t \rightarrow \infty) \quad (16)$$

where $C(t)$ is a value that only depends on time. This assumption implies that the shape of the probability distribution at the barrier deformation as a function of the velocity v is constant, and only its height varies with time. This statement is certainly valid in the overdamped motion were the equilibrium in velocity is established very rapidly. However, the calculations presented in the appendix prove that expression (16) is still applicable outside the overdamped regime. The reason for this is that since x_b is far away from the initial deformation, the time needed for the probability distribution W to reach the fission barrier is large enough for the velocity to equilibrate. Thus, by the time when $W_n(x = x_b, v, t)$ starts to noticeably differ from zero, the probability distribution as a function of the velocity coordinate has already attained the asymptotic shape $W_n(x = x_b, v, t \rightarrow \infty)$. Integrating equation (16) over the whole velocity interval and defining:

$$W(x = x_b, t) = \int_{-\infty}^{+\infty} W(x = x_b, v, t) dv \quad (17)$$

We can express $C(t)$ as:

$$C(t) = \frac{\int_{-\infty}^{+\infty} W_n(x = x_b, v, t) dv}{\int_{-\infty}^{+\infty} W_n(x = x_b, v, t \rightarrow \infty) dv} = \frac{W_n(x = x_b, t)}{W_n(x = x_b, t \rightarrow \infty)} \quad (18)$$

Introducing equation (16) into equation (15) and using equation (18) leads to:

$$\Gamma_f(t) \approx \frac{W_n(x = x_b, t)}{W_n(x = x_b, t \rightarrow \infty)} \Gamma_f^K \quad (19)$$

The second approximation consists on expressing the shape of the in-growth function at the fission barrier $W_n(x = x_b, t)$ in equation (19) by equations (7) and (8), derived for the parabolic potential:

$$\Gamma_f(t) \approx \frac{W^{par}(x = x_b, t)}{W^{par}(x = x_b, t \rightarrow \infty)} \Gamma_f^K \quad (20)$$

Note, that we replaced the normalised probability W_n^{par} by the unnormalised quantity W^{par} in equation (20), because in the case of the parabolic potential the probability distribution is confined, and thus $\int_{-x_b}^{+\infty} W(x, t) \approx \int_{-\infty}^{+\infty} W(x, t)$. Implementing equations (7) and (8) in equation (20) results in an analytical expression for $\Gamma_f(t)$.

Due to the classical nature of the FPE equation, the initial behaviour predicted by equation (20) should not be considered since for $t = 0$ equation (8) gives $\sigma = 0$. Being a quantum-mechanical system, the initial probability distribution of the nucleus as a function of the position and the momentum coordinate has a finite width. As initial condition of the problem we selected the zero-point motion at the ground-state deformation. The zero-point motion is taken into account by shifting the time scale by a certain amount t_0 . For the under-damped case ($\beta < 2\omega_l$), the deformation and the momentum coordinate saturate at about the same time. Therefore, the time shift needed for the probability distribution to reach the width of the zero-point motion in deformation space is equal to the time that the average energy of the collective degree of freedom needs to reach the value $\frac{1}{2}\hbar\omega_l$ associated to the zero-point motion:

$$t_0^{under} = \frac{1}{\beta} \ln \left(\frac{2T}{2T - \hbar\omega_l} \right) \quad (21)$$

In the over-damped regime ($\beta \geq 2\omega_l$), the momentum coordinate saturates very fast, while the population of the deformation space results from a diffusion process. Neglecting the influence of the potential on the diffusion process, which is anyhow small in the range of the zero-point motion, the solution of the Fokker-Planck equation gives the following time evolution for the variance of the probability distribution in the deformation coordinate [53]:

$$\sigma_{\bar{x}}^2(t) = \frac{2T}{\mu\beta} t \quad (22)$$

Replacing in equation (22) $\sigma_{\bar{x}}^2(t)$ by the value of the variance associated to the zero-point motion $\frac{\hbar}{2\mu\omega_l}$ results in:

$$t_0^{over} = \frac{\hbar\beta}{4\omega_l T} \quad (23)$$

The time shift t_0 is already included in the calculations shown in figure 2 and in table 1.

The analytical expression that results from combining equations (7) and (8) with equation (20), represents a very adequate description of $\Gamma_f(t)$ as can be seen in figure 2a), where this

function (dashed line) is compared to the numerical calculation (full line). Moreover, the comparison of this approximation with the numerical solution of the FPE for $\beta \leq 2\omega_l$ presented in the appendix demonstrates that this approximation quite well reproduces the exact solution of the FPE for the critical damping and the underdamped regime, as well. This may be understood by the following arguments. For given values of β and T , the time behaviour of the exact solution of the FPE is mainly governed by two parameters: the frequency ω_l at the ground state and the barrier deformation x_b . The formulation we present here uses realistic values of ω_l and x_b in the harmonic approximation, whereas the absolute value of the fission-decay width is taken from Kramers's stationary solution for the realistic potential shape (full line in figure 1a). This explains the good agreement of this formulation with the numerical calculation. This approximation is suited to be used in complex nuclear-reaction codes, where solving the Fokker-Planck equation numerically would introduce a not affordable additional computing time.

We would like to stress that the proposed approximate in-growth function, deduced from the solution of the Fokker-Planck equation of the parabolic potential, represents the practically complete suppression of the initial fission-decay width in a realistic way, because it directly considers the physical process of gradually populating the deformation space. Alternative formulations based on parameterizing the rather complex shape of the in-growth function by less adequate functional forms, like the Fermi function, might miss this feature, which will be shown below to be very important.

3.4 Detailed view on the model calculations

It is very illustrative to compare how the excitation energy with which the nucleus crosses the saddle point changes in the model calculation when using the different approximations for describing $I_j(t)$. Let us first consider the unrealistic case, where there is no upper limit for the initial temperature of the sequential decay. Figure 3 depicts the excitation energy of the nucleus at the saddle point against the initial excitation energy of the prefragment for the fission events produced in the reaction of ^{238}U at 1.4 GeV in a lead target. Calculation 3a) corresponds to the step-function description with $\beta = 2 \cdot 10^{21} \text{ s}^{-1}$, calculation 3b) to the exponential-like description with $\beta = 4 \cdot 10^{21} \text{ s}^{-1}$, and 3c) to the proposed analytical solution of the FPE with a parabolic nuclear potential and $\beta = 2 \cdot 10^{21} \text{ s}^{-1}$. These values of β are the ones required to reproduce the total nuclear fission cross section of this reaction by the different descriptions.

Mid-peripheral heavy-ion collisions allow producing nuclei with excitation energies that are far beyond the onset of multifragmentation [37]. Nuclear dynamics in this range of excitation energies is the subject of current research. As presented in reference [43], the analysis of the isotopic distributions of heavy projectile fragments from the reactions of a ^{238}U beam in a lead target gave some evidence that the initial temperature of the last stage of the reaction, the evaporation cascade, is limited to a universal value of approximately 5.5 MeV. The interpretation of this effect relies on the onset of a simultaneous break-up process for systems whose temperature after the abrasion is larger than 5.5 MeV. In reference [43], the simultaneous break-up stage has been modelled in a quite rough way that however shows a very good agreement with the experimental data. If the temperature after abrasion exceeds the freeze-out temperature of 5.5 MeV, the additional energy is used for the simultaneous emission of nucleons or small clusters. The number of protons and neutrons emitted is assumed to conserve the N -over- Z ratio of the projectile spectator, and an amount of about 20 MeV per nuclear mass unit emitted is released. This last quantity is still under investigation. Nevertheless, its effect on the fission cross sections is very small. After the spontaneous

emission, the piece left of the projectile spectator then undergoes the sequential decay where fission and particle evaporation are competing processes.

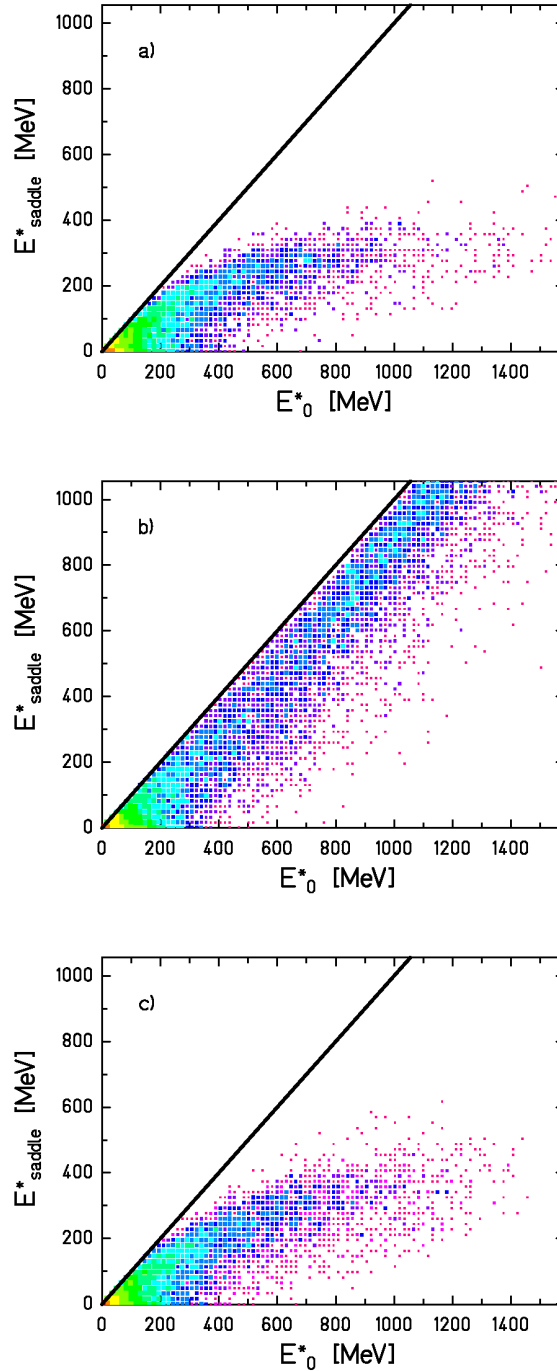


Figure 3: Calculations performed with ABRABLA without including the break-up stage. They represent the excitation energy at fission versus the excitation energy of the prefragment after abrasion for the fission events obtained in the reaction of 1.4 GeV ^{238}U on a lead target. a) Calculation performed with $\Gamma_f(t)$ as a step function and $\beta = 2 \cdot 10^{21} \text{ s}^{-1}$. b) Calculation with $\Gamma_f(t) \propto (1 - e^{-t/\tau})$ and $\beta = 4 \times 10^{21} \text{ s}^{-1}$. c) Calculation carried out with equation (20) taking $W^{par}(x = x_b, t)$ from equations (7) and (8) and $\beta = 2 \cdot 10^{21} \text{ s}^{-1}$. In all cases we have used $\hbar\omega_1 = 1 \text{ MeV}$. The straight lines represent the upper limit for the excitation energy at fission.

The same set of calculations as in figure 3 but including the break-up stage is shown in figure 4. By comparing figure 3 and figure 4, one immediately recognizes that the effect of the

break-up process on the calculation performed with the exponential-like description for $\Gamma_j(t)$ is much more drastic than for the two other calculations. The too early onset of fission introduced by the exponential-like in-growth function implies that fission at high excitation energies is not suppressed by dissipation in this calculation. Fission reaches to such high excitation energies, that it is rather constricted by the break-up mechanism. On the contrary, the calculations performed with the step function and with the analytical solution of the FPE illustrate that dissipation considerably inhibits the fission decay channel for excitation energies at fission above 300 MeV and, therefore, the effect of the break-up process is significantly smaller. Figure 2b) shows that for the analytical solution of the FPE the fission probability sets in earlier than for the step function, leading to a larger amount of fissioning systems with initial excitation energies E_0^* beyond 800 MeV, as can be seen comparing figures 3a) and 3c). As a result, the break-up stage has a stronger effect in this case than in the case of the step function.

The strength of the effects of the simultaneous break-up in the deexcitation process can also be observed from the cross sections of table 1. When the exponential-like description of $\Gamma_j(t)$ is used, the calculated cross sections differ considerably, depending on whether the break-up stage is included or not in the calculation. In contrast, the calculated cross sections obtained by applying the analytical solution of the FPE do not present such a remarkable difference, and the ones calculated using the step function are hardly affected by this feature.

The 45-degree straight lines depicted on the six spectra of figures 3 and 4 correspond to the upper limit for the excitation energy at fission. Both, the calculation performed with the step function on figure 3a) and the calculation with the analytical solution of the FPE on figure 3c), show that this line starts to be depopulated at initial excitation energies of approximately 150 MeV, indicating that from these excitation energies on the transient time is longer than the decay time for particle emission. That means that prefragments with initial excitation energies higher than ≈ 150 MeV can only fission after cooling down by particle evaporation.

3.5 Conclusion

The previous discussion has shown that the step function described by equation (3), although it appears to be a rather crude approximation, better describes the effects of dissipation on the fission decay width than the exponential-like function of equation (4). It also leads to a strong suppression of fission at high excitation energies in quite good agreement with the more realistic description of the fission width given by the analytical solution of the FPE for a parabolic nuclear potential. When the step function is used, the experimental data selected are reproduced with a reduced dissipation coefficient of $\beta = 2 \cdot 10^{21} \text{ s}^{-1}$. The same value of $\beta = 2 \cdot 10^{21} \text{ s}^{-1}$ is obtained when the more realistic description of $\Gamma_j(t)$ based on the analytic solution of the FPE is applied. From figure 2b) one would expect that the analytical solution of the FPE requires a larger value of β to describe the experimental data than the step function, but as was explained before, the break-up mechanism suppresses the additional fission events at high excitation energies and leads to very similar fission cross sections. The latter comment demonstrates that, due to the possible existence of fission events at very high excitation energies, any conclusion on dissipation cannot be drawn without explicitly considering the thermal stability of nuclei against break-up.

Our investigation does not allow a direct conclusion on the temperature dependence of the dissipation coefficient β , but it reveals the difficulty in deducing such an effect. The different distributions of excitation energies at fission found in the calculations shown in figures 3 and 4 prove that this analysis strongly depends on the in-growth function assumed for $\Gamma_j(t)$. For

instance, the inhibition of fission at high excitation energies obtained with the analytical solution and the step function could be achieved with the exponential-like in-growth function as well by setting very high values of β at high temperatures. Therefore, it cannot be excluded that the indications for strong increase of nuclear viscosity with increasing temperature drawn in several publications [54, 55] might be attributed to the unrealistic exponential-like in-growth function used in the analysis.

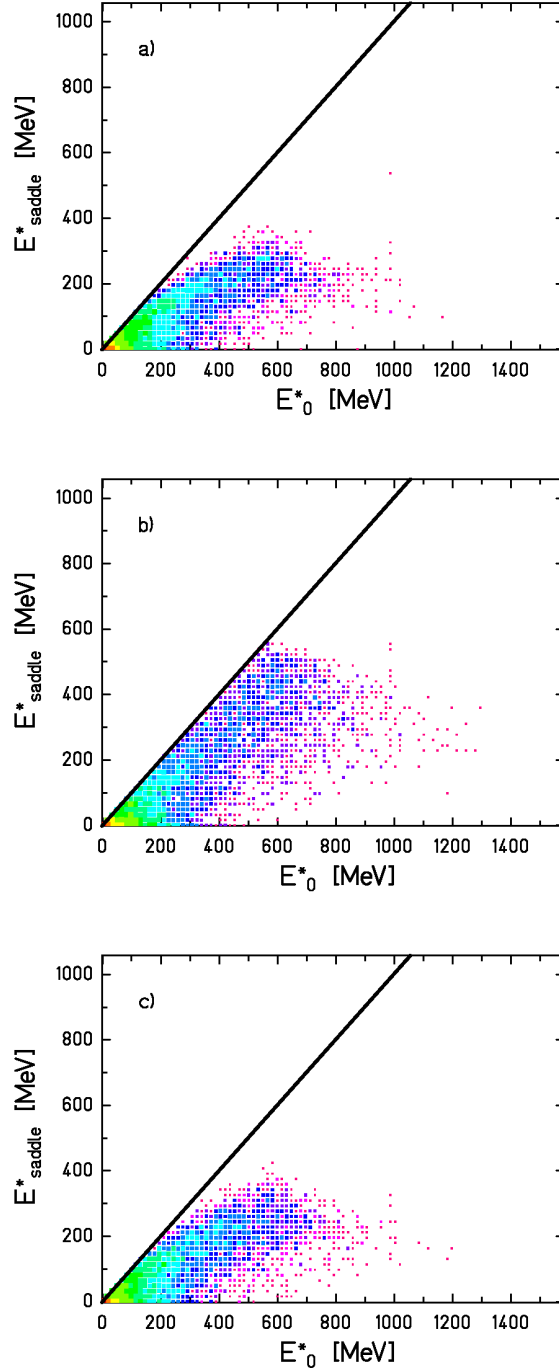


Figure 4: The same calculations as in figure 3 but including the break-up stage in ABRABLA. The cluster plots represent the excitation energy at fission versus the excitation energy of the prefragment before the break-up stage for the fission events obtained in the reaction of 1.4 GeV ^{238}U on a lead target.

The description of $\Gamma_f(t)$ that reproduces the present data is influenced by transient effects only for excitation energies at saddle within the interval $150 \text{ MeV} < E_{saddle}^* < 350 \text{ MeV}$. Above this

range, our experimental data are not sensitive to the strength of β since at excitation energies above 350 MeV fission is almost completely inhibited. Therefore, an eventual increase of the dissipation coefficient for excitation energies larger than 350 MeV would not be observable. At excitation energies below 150 MeV, the statistical decay times are appreciably longer than the dynamical time scale, represented by the transient time, as long as the value of β remains in a certain range, making the experimental observables rather insensitive to the transient time. The Kramers factor implies a reduction of the fission width that should have some effect on the measured data at these low excitation energies. Nevertheless, the observation of such an effect is much more difficult than the observation of the total suppression of fission by the transient time, because it requires a very accurate knowledge of the other model parameter, in particular of the level density.

The nuclei that contribute to the fission cross sections studied in this work extend over a broad range of masses, charges and excitation energies at the saddle point. Hence, according to equation (2) and assuming $\hbar\omega_I = 1$ MeV [44], the value of β found corresponds to a distribution of transient times with the mean value $\tau_f \approx (1.7 \pm 0.4) \cdot 10^{-21}$ s. Because our results are based on the analysis of fission cross sections, they are only sensitive to dissipation in the small deformation range from the ground state to the saddle point. The value of $\beta = 2 \cdot 10^{21} \text{ s}^{-1}$ obtained from our analysis coincides with the value found in reference [28], where total fission cross sections as well as the widths of the charge distributions and velocities of the fission residues from the reaction Au (800-A MeV) + p are analysed with the step-function description of $\Gamma_f(t)$. Other work [16, 18, 52] sensitive to the same deformation range is consistent with our conclusions, although often only upper limits for the transient time or the dissipation coefficient could be deduced. Our result for τ_f entails that for nuclei with excitation energies lower than 100 MeV the transient time is still a too tiny effect to have observable influence on the fission-decay width. Experiments need to populate higher excitation energies in order to be sensitive to transient effects on the way to the saddle point.

The quantitative value deduced for the dissipation coefficient remains model dependent to a certain degree. Nevertheless, variations of the most critical model parameters by reasonable amount: excitation energy of the prefragments by 30%, freeze-out temperature by 20 % and excitation energy reduction per mass loss in the break-up stage by a factor of two led to variations of the deduced transient time well inside the uncertainty range given. The most important achievement of the present work, however, is the detailed discussion of an experimental method suited for the study of dissipation at small deformation and the appropriate modelling of dissipation effects in nuclear-reaction codes.

4. Summary

Peripheral heavy-ion collisions at relativistic energies are a very suitable tool for investigating dissipation, because highly excited nuclei are produced with initial conditions that closely correspond to the assumptions of the theoretical model of Grangé and Weidenmüller. We analysed the nuclear-induced total fission cross sections of ^{238}U at 1-A GeV on two different heavy targets by means of the Monte-Carlo code ABRABLA. We implemented in this code the two most widely used descriptions for the time dependence of the fission-decay width, a step function and an exponential-like in-growth function, and in addition a highly realistic description based on the analytical solution of the FPE when the nuclear potential is approximated by a parabola. The reduced dissipation coefficient β deduced depends strongly on whether the step function, the exponential-like in-growth function or the analytical approximation is used. Consequently, in order to interpret any result on the magnitude of β , the description used for the time dependence of the fission width must be considered. A

Careful analysis of the exponential-like in-growth function has shown that it fails in reproducing the total suppression of fission at the beginning of the deexcitation process that is expected theoretically. This description of $\Gamma_f(t)$ would imply that at high excitation energies the fission process is not suppressed by dissipation. On the contrary, the step-function approximation and the proposed analytical description show a quite similar behaviour. This indicates that the suppression of the fission decay width during the initial time span is needed to account for dissipation effects in a proper way. The analysis performed in this work clearly demonstrates that transient effects in fission are accessible to experimental investigations. Using the analytical solution of the FPE given by equations (20), (7) and (8), the experimental data are reproduced when $\beta = 2 \cdot 10^{21} \text{ s}^{-1}$. This value of β corresponds to a transient time of $\tau_f \approx (1.7 \pm 0.4) \cdot 10^{-21} \text{ s}$.

Acknowledgment

We thank O. Yordanov for the assistance in using the FEMLAB code. This work was supported by the European Commission under the programme "Access to Research Infrastructure Action of the Improving Human Potential" contract EC-HPRI-CT-1999-00001 and under the ECT* 'STATE' contract.

Appendix: Treatment of fission as a dissipative process in ABRABLA

In this appendix we document in detail how dissipation is described in the evaporation part of the Monte-Carlo code ABRABLA [39, 40]. The main evaporation channels we consider are neutron, proton and alpha-particle emission. Each of these decay modes is represented by a partial decay width Γ_ν , which is related to the partial lifetime $\tau_\nu = \hbar / \Gamma_\nu$. In the following, we distinguish only between two decay channels, particle evaporation, which groups neutron, proton and alpha-particle emission, and fission. The particle-decay mode is represented by the decay width

$$\Gamma_p = \sum_\nu \Gamma_\nu \quad (\text{A1})$$

and the corresponding partial particle decay time τ_p is defined by

$$\frac{1}{\tau_p} = \sum_\nu \frac{1}{\tau_\nu} \quad (\text{A2})$$

While the particle-decay widths do not explicitly depend on time, dissipation effects lead to a time-dependent fission width $\Gamma_f(t)$. Therefore, at the beginning of each step of the deexcitation cascade one has to consider the time elapsed during the previous stages. Physically this means that, while particles are emitted, the probability distribution in deformation space becomes broader, and at each step of the deexcitation cascade the distribution "remembers" its current width. Accordingly, in every step n we have to evaluate the fission width $\Gamma_f(t)$ with a time variable whose initial value increases with each step as

$$t_{sum}^n = \sum_i^{n-1} \tau_i \quad (\text{A3})$$

Here τ_i represents the average decay time at the corresponding step and includes the mean particle decay time τ_p and the mean decay time for fission $\tau_{fission}$. If this feature is not taken into account, fission would set in at a time that is larger than the transient time τ_f . This fact explains why a previous version of ABRABLA underestimated the cross-sections of table 1 [38].

For describing the shape of $\Gamma_f(t)$ we incorporated in the code the two approximations represented by equations (3) and (4) described in section 1 and the more sophisticated case given by equations (20), (7) and (8) of section 3. In all cases the stationary value of the fission width is

$$\Gamma_f^{K,n} = \Gamma_f^{BW,n} \cdot K \quad (\text{A4})$$

where $\Gamma_f^{BW,n}$ is the fission width given by the transition-state model [1] at the step n and K is the Kramers factor already introduced in equation (1) of section 1. Detailed formulations of the three cases are given below.

A1. Description of $\Gamma_f(t)$ by a step function

As shown in section 1, the fission width can be described by a step function that sets in to the stationary value given by equation (A4) at the transient time τ_f .

Let I_0 be the number of nuclei available at the beginning of a certain step n . For the time interval $t_{sum}^n < t < \tau_f$, particle emission is the only deexcitation channel available and the number of nuclei that decay in that step n is

$$I_0 \cdot (1 - \exp(-(\tau_f - t_{sum}^n) / \tau_p^n)) \quad (\text{A5})$$

The upper index n indicates that these quantities differ from step to step. For $t \geq \tau_f$, fission is also possible, and the additional number of nuclei that decay by particle emission at the same step is

$$I_0 \cdot \exp(-(\tau_f - t_{sum}^n) / \tau_p^n) \cdot \frac{\Gamma_p^n}{\Gamma_p^n + \Gamma_f^{K,n}} \quad (\text{A6})$$

where the quantity $I_0 \cdot \exp(-(\tau_f - t_{sum}^n) / \tau_p^n)$ represents the nuclei that survived particle emission before τ_f . Similarly, the number of nuclei that fission after τ_f is

$$I_0 \cdot \exp(-(\tau_f - t_{sum}^n) / \tau_p^n) \cdot \frac{\Gamma_f^{K,n}}{\Gamma_p^n + \Gamma_f^{K,n}} \quad (\text{A7})$$

The total probability for particle evaporation at a step n can be obtained by normalizing the total number of decays to the initial number of nuclei I_0 leading to the expression

$$P_p^n = (1 - \exp(-(\tau_f - t_{sum}^n) / \tau_p^n)) + \exp(-(\tau_f - t_{sum}^n) / \tau_p^n) \cdot \frac{\Gamma_p^n}{\Gamma_p^n + \Gamma_f^{K,n}} \quad (\text{A8})$$

and the total probability for fission is

$$P_f^n = \exp(-(\tau_f - t_{sum}^n) / \tau_p^n) \cdot \frac{\Gamma_f^{K,n}}{\Gamma_p^n + \Gamma_f^{K,n}} \quad (\text{A9})$$

This formulation is similar but more consistent than the approach proposed previously in [44] and [46].

A2. Description of $\Gamma_f(t)$ by an exponential in-growth function

Another possibility to describe the time dependence of the fission width $\Gamma_f(t)$ is an exponential in-growth function, equation (4) of section 1. In this case, the procedure is different than in the previous one because $\Gamma_f(t)$ increases continuously with time.

The decay rate at a step n can be written as:

$$\left(\frac{dI}{dt}\right)_n = -\left[\frac{\Gamma_p^n}{\hbar} + \frac{\Gamma_f^n(t)}{\hbar}\right] \cdot I^n(t) = -\left[\frac{\Gamma_p^n}{\hbar} + \frac{\Gamma_f^{K,n}}{\hbar} (1 - \exp(-\frac{t+t_{sum}^n}{\tau}))\right] \cdot I^n(t) \quad (A10)$$

By integrating equation (A10) we obtain an analytical expression for $I^n(t)$

$$I^n(t) = I_0 \cdot \exp(-\frac{\Gamma_p^n + \Gamma_f^{K,n}}{\hbar} t) \cdot \left[\exp(-\frac{\Gamma_f^{K,n} \cdot \tau}{\hbar} \cdot \exp(-\frac{t+t_{sum}^n}{\tau})) \right] \quad (A11)$$

Substituting equation (A11) in (A10) we obtain an analytical expression for the decay rate $(dI(t)/dt)_n$ of the nucleus that includes all possible particle decay channels and the already mentioned time dependence of Γ_f . After evaluating $(dI(t)/dt)_n$ for the corresponding step, we sample from $(dI(t)/dt)_n$ the decay time and finally calculate the value of $\Gamma_f(t)$ at that decay time. The decay channel is then determined by a Monte-Carlo selection with the weights $\Gamma_f(t)/\Gamma_{total}$ for fission and $\Gamma_\nu/\Gamma_{total}$ for the emission of the particle ν .

A3. Description of $\Gamma_f(t)$ by the analytical solution of the FPE for a parabolic nuclear potential

As shown by the dashed line in figure 2a) of section 3, the analytical solution of the FPE when the nuclear potential is approximated by a parabola gives a much more realistic description of the time dependence of the fission rate $\lambda_f(t)$ than the step function and the exponential-like in-growth function. This analytical expression for the fission rate can be obtained by using equation (20) and taking $W^{par}(x=x_b, t)$ from equations (7) and (8). Actually, the method [56] we use to include this description of $\Gamma_f(t)$ in the evaporation code is applicable for any function representing $\Gamma_f(t)$. We first divide the time interval $0 < t < 1.5 \cdot \tau_f$ (for $t = 1.5 \cdot \tau_f$ the fission width has already reached its stationary value) in small subintervals

of length $L = \frac{1.5 \cdot \tau_f}{50}$. If we are inside a certain step n , we define the value of the fission decay width as the quantity

$$\Gamma_{f,i}^n = \frac{\Gamma_f^n(t_{tot} + i \cdot L) + \Gamma_f^n(t_{tot} + (i+1) \cdot L)}{2} \quad (A12)$$

with $i = 0$ at the beginning of each step and $t_{tot} = t_{sum}^n + t_0$, where t_0 accounts for the zero point motion and is given by equation (21) in the underdamped regime and by equation (23) in the

overdamped regime. This value of the fission decay width is used to evaluate the decay probability inside this small subinterval i

$$P_{decay}^i = 1 - \exp\left(-\frac{L}{\tau^i}\right) \quad (\text{A13})$$

with

$$\frac{1}{\tau^i} = \frac{\Gamma_p^n}{\hbar} + \frac{\Gamma_{f,i}^n}{\hbar} \quad (\text{A14})$$

By means of a Monte-Carlo selection we establish whether the nucleus decays inside this time subinterval i or not. If no decay takes place, we evaluate again expression (A12) for the next subinterval $i+1$ and so on, until the nucleus decays. The decay channel is then determined by a further Monte-Carlo selection with the weights Γ_p^n and $\Gamma_{f,i}^n$.

As shown by equations (7) and (8) of section 3, in this case we have an additional dependence of $\Gamma_f(t)$ on the deformation at the fission barrier x_b , on the reduced mass μ and on the frequency of the system at the ground state ω_l . Considering that

$$\mu\omega_l^2 = 2K_1 \quad (\text{A15})$$

where K_l is the stiffness of the parabolic nuclear potential, the implementation of this description in the evaporation code requires determining the saddle point deformation x_b and the stiffness K_l of the different nuclei that are produced during the deexcitation cascade. For the saddle point deformation x_b we use the expression taken from [57]

$$x_b = \frac{7}{3}y - \frac{938}{765}y^2 + 9.499768y^3 - 8.050944y^4 \quad (\text{A16})$$

where $y = 1-\alpha$ and α is the fissility parameter. For the stiffness K_1 , we use the liquid-drop-model predictions of reference [58]

$$K_1 = \left[7.1776 \left(1 - 1.7826 \left(\frac{A-2Z}{A} \right)^2 \right) A^{2/3} - 0.1464 \frac{Z^2}{A^{1/3}} \right] \text{MeV} \quad (\text{A17})$$

We should remark that for the three descriptions considered, when calculating t_{sum}^n , we express the particle decay time and the fission decay time by the average decay times τ_p and $\tau_{fission}$ instead of sampling these quantities from a statistical decay-time distribution. In spite of this approximation, our treatment of the decay cascade is more realistic than previous formulations. For example, in reference [45] several analytical expressions for the probabilities of the diverse decay channels are given considering the step function and the exponential in-growth function to describe the form of $\Gamma_f(t)$. However, this is done under the simplifying assumption that the total decay widths are unchanged from one step to the next in the decay cascade. In [13] the exponential-like in-growth function is used, but the total decay time at each step of the cascade is considered to be ruled uniquely by the neutron-decay life time at that step, while the influence on the life time introduced by the other possible decay channels is not considered.

As already briefly reported in reference [33], we have compared the proposed analytical approximation for the time-dependent fission width with the numerical solution of the FPE

for $\Gamma_f(t)$ *. As can be seen in figures A1a) and A1b), this analytical approximation quite well reproduces the exact solution for the critical damping ($\beta = 2 \cdot 10^{21} \text{ s}^{-1}$) and the slightly under-damped motion ($\beta = 1 \cdot 10^{21} \text{ s}^{-1}$). Even in the strongly under-damped case ($\beta = 0.5 \cdot 10^{21} \text{ s}^{-1}$), the onset of the fission decay and the oscillations are reproduced quite well as demonstrated in figure A1c), although the absolute magnitude of the fission rate is somewhat underestimated. Figures 2a) and A1 demonstrate the validity of this new approximation for $\Gamma_f(t)$ in the overdamped as well as in the underdamped regime. The proposed description of the time-dependent fission-decay width may substitute less realistic formulations in nuclear-model codes, leading to more reliable conclusions on nuclear dissipation.

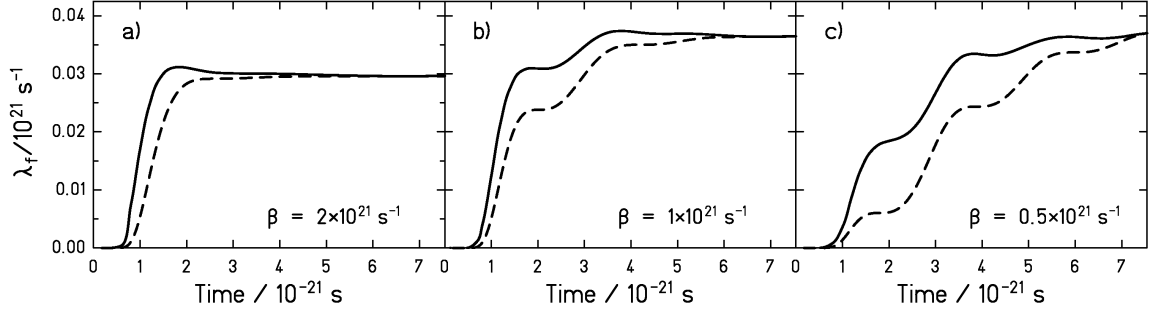


Figure A1: Fission rate $\lambda_f(t) = \Gamma_f(t) / \hbar$ as a function of time for three different values of the reduced dissipation coefficient β for ^{238}U at $T = 3 \text{ MeV}$. The solid line is the numerical solution of the FPE while the dashed line is calculated using equation (20) with $W_n(x=x_b, t, \beta)$ taken from equations (7) and (8). The initial conditions correspond to the zero-point motion (see main text). Figure taken from ref. [33].

* The numerical solutions of the FPE were obtained with the software package FEMLAB (Comsol AB, Stockholm)

References

- [1] N. Bohr and J. A. Wheeler, *Phys. Rev.* 56 (1939) 426
- [2] H. A. Kramers, *Physika* VII 4 (1940) 284
- [3] *The Fokker-Planck Equation*, H. Risiken, Springer, Berlin, ISBN 0-387-50498-2
- [4] D. Hilscher, E. Holub, U. Jahnke, H. Orf, and H. Rossner, *Proc. of the 3rd Adriatic Europhysics Conference on the Dynamics of Heavy-Ion Collisions*, Hvar, Croatia, Yugoslavia, May 25-30 (1981) 225
- [5] A. Gavron, J. R. Beene, B. Cheynis, R. L. Ferguson, F. E. Obenshain, F. Plasil, G. R. Young, G. A. Petitt, M. Jääskeläinen, D. G. Sarantites, and C. F. Maguire, *Phys. Rev. Lett.* 47 (1981) 1255. Errata: *Phys. Rev. Lett.* 48 (1982) 835
- [6] P. Grangé, L. Jun-Qing, and H. A. Weidenmüller, *Phys. Rev. C* 27 (1983) 2063
- [7] K.-H. Bhatt, P. Grangé, and B. Hiller, *Phys. Rev. C* 33 (1986) 954
- [8] J. Blocki, Y. Boneh, J. R. Nix, J. Randrup, M. Robel, A. J. Sierk, and W. J. Swiatecki, *Ann. Phys.* 113 (1978) 330
- [9] W. Nörenberg, *Nucl. Phys. A* 409 (1983) 191c
- [10] H. Hofmann, *Phys. Rep.* 284 (1997) 137
- [11] H. Rossner, D. J. Hinde, J. R. Leigh, J. P. Lestone, J. O. Newton, J. X. Wie, and S. Elfström, *Phys. Rev. C* 45 (1992) 719
- [12] D. J. Hinde, D. Hilscher, H. Rossner, B. Gebauer, M. Lehmann, and M. Wilpert, *Phys. Rev. C* 45 (1992) 1229
- [13] R. Butsch, D. J. Hofman, C. P. Montoya, P. Paul, and M. Thoennessen, *Phys. Rev. C* 44 (1991) 1515
- [14] H. Ikezoe, N. Shikazono, Y. Nagame, Y. Sugiyama, Y. Tomita, K. Ideno, A. Iwamoto, and T. Ohtsuki, *Phys. Rev. Lett. C* 42 (1990) 342
- [15] J. P. Lestone, J. R. Leigh, J. O. Newton, D. J. Hinde, J. X. Wei, J. X. Chen, S. Elfstrom, and D. G. Popescu, *Phys. Rev. Lett.* 67 (1991) 1078
- [16] S. K. Hui, C. R. Bhuinya, A. K. Ganguly, N. Madhavan, J. J. Das, P. Sugathan, D. O. Kataria, S. Murlithar, L. T. Baby, V. Tripathi, A. Jhingan, A. K. Sinha, P. V. Madhusudhana Rao, N. V. S. V. Prasad, A. M. Vinodkumar, R. Singh, M. Thoennessen, and G. Gervais, *Phys. Rev. C* 62 (2000) 054604
- [17] I. Diószegi, *Phys. Rev. C* 64 (2001) 019801
- [18] L. G. Moretto, K. X. Jing, R. Gatti, G. J. Wozniak, and R. P. Schmitt, *Phys. Rev. Lett.* 75 (1995) 4186
- [19] F. Goldenbaum, M. Morjean, J. Galin, E. Lienard, B. Lott, A. Peghaire, Y. Perier, M. Chevallier, D. Dauvergne, R. Kirsch, J. C. Poizat, J. Remillieux, C. Cohen, A. L'Hoir, G. Prevot, D. Schmaus, J. Dural, M. Toulemonde, and D. Jacquet, *Phys. Rev. Lett.* 82 (1999) 5012
- [20] D. Hilscher and H. Rossner, *Ann. Phys. Fr* 17 (1992) 471
- [21] D. J. Hofman, B. B. Back, and P. Paul, *Phys. Rev. C* 51 (1995) 2597
- [22] J. Wilczynski, K. Siwek-Wilczynska, and H. W. Wilschut, *Phys. Rev. C* 54 (1996) 325
- [23] H. van der Ploeg, J. C. S. Bacelar, I. Diószegi, G. van't Hof, and A. van der Woude, *Phys. Rev. Lett.* 75 (1995) 970
- [24] I. Diószegi, N. P. Shaw, A. Bracco, F. Camera, S. Tettoni, M. Mattiuzzi, and P. Paul, *Phys. Rev. C* 63 (2001) 014611
- [25] J. Velkovska, C. R. Morton, R. L. McGrath, P. Chung, and I. Diószegi, *Phys. Rev. C* 59 (1999) 1506
- [26] A. V. Karpov, P. N. Nadtochy, D. V. Vanin, and G. D. Adeev, *Phys. Rev. C* 63 (2001) 054610
- [27] P. Fröbrich and I. I. Gontchar, *Nucl. Phys. A* 563 (1993) 326
- [28] J. Benlliure, P. Armbruster, M. Bernas, A. Boudard, T. Enqvist, R. Legrain, S. Leray, F. Rejmund, K.-H. Schmidt, C. Stephan, L. Tassan-Got, and C. Volant, *Nucl. Phys. A* 700 (2002) 469

-
- [29] K. X. Jing, L. G. Moretto, A. C. Veeck, N. Colonna, I. Lhenry, K. Tso, K. Hanold, W. Skulski, Q. Sui, and G. J. Wozniak, Nucl. Phys. A645 (1999) 203
- [30] B. Lott, F. Goldenbaum, A. Böhm, W. Bohne, T. von Egidy, P. Figuera, J. Galin, D. Hilscher, U. Jahnke, J. Jastrzebski, M. Morjean, G. Pausch, A. Péghaire, L. Pienkowski, D. Polster, S. Proschitzki, B. Quednau, H. Rossner, S. Schmid, and W. Schmid, Phys. Rev. C 63 (2001) 034616
- [31] A. V. Karpov, P. N. Nadtochy, D. V. Vanin, and G. D. Adeev, Phys. Rev. C 63 (2001) 054610
- [32] V. P. Aleshin, M. Centelles, X. Vinas, and N. G. Nicolis, Nucl. Phys. A 679 (2001) 441
- [33] B. Jurado, K.-H. Schmidt, and J. Benlliure, Phys. Lett. B 533 (2003) 186
- [34] M. de Jong, A. V. Ignatyuk, and K.-H. Schmidt, Nucl. Phys. A 613 (1997) 435
- [35] F. Goldenbaum, W. Bohne, J. Eades, T. von Egidy, P. Figuera, H. Fuchs, J. Galin, Ye. S. Golubeva, K. Gulda, D. Hilscher, A. S. Iljinov, U. Jahnke, J. Jastrzebski, W. Kurcewicz, B. Lott, M. Morjean, G. Pausch, A. Peghaire, L. Pienkowski, D. Polster, S. Proschitski, B. Quednau, H. Rossner, S. Schmid, W. Schmid, and P. Ziem, Phys. Rev. Lett. 77 (1996) 1230
- [36] P. Hofmann, A. S. Iljinov, Y. S. Kim, M. V. Mebel, H. Daniel, P. David, T. von Egidy, T. Haninger, F. J. Hartmann, J. Jastrzebski, W. Kurcewicz, J. Lieb, H. Machner, H. S. Plendl, G. Riepe, B. Wright, and K. Ziock, Phys. Rev. C 49 (1994) 2555
- [37] J. Pochodzalla and W. Trautmann, preprint to appear in “Isospin Physics in Heavy-Ion Collisions at Intermediate Energies” Nova Science Publishers, Inc.
<http://www.arxiv.org/abs/nucl-ex/0009016>
- [38] Th. Rubehn, R. Bassini, M. Begemann-Blaich, Th. Blaich, A. Ferrero, C. Groß, G. Immé, I. Iori, G. J. Kunde, W. D. Kunze, V. Lindenstruth, U. Lynen, T. Möhlenkamp, L. G. Moretto, W. F. J. Müller, B. Ocker, Pochodzalla, G. Raciti, S. Reito, H. Sann, A. Schüttauf, W. Seidel, V. Serfling, W. Trautmann, A. Trzcinski, G. Verde, A. Wörner, E. Zude, and B. Zwieglinski, Phys. Rev. C 53 (1996) 3143
- [39] J.-J. Gaimard and K.-H. Schmidt, Nucl. Phys. A 531 (1991) 709
- [40] A. R. Junghans, M. de Jong, H.-G. Clerc, A. V. Ignatyuk, G. A. Kudyaev, and K.-H. Schmidt, Nucl. Phys. A 629 (1998) 635
- [41] K.-H. Schmidt, T. Brohm, H.-G. Clerc, M. Dornik, M. Fauerbach, H. Geissel, A. Grewe, E. Hanelt, A. Junghans, A. Magel, W. Morawek, G. Münzenberg, F. Nickel, M. Pfützner, C. Scheidenberger, K. Sümmerer, D. Vieira, B. Voss, and C. Ziegler, Phys. Lett. B 300 (1993) 313
- [42] J. C. Hubele, Ph. D. Thesis, University of Frankfurt, Germany, (1991)
- [43] K.-H. Schmidt, M. V. Ricciardi, A. Botvina, and T. Enqvist, Nucl. Phys. A 710 (2002) 157
- [44] E. M. Rastopchin, S. I. Mul’gin, Yu. B. Ostapenko, V. V. Pashkevich, M. I. Svirin, and G. N. Smirenkin, Yad. Fiz. 53 (1991) 1200 [Sov. J. Nucl. Phys. 53 (1991) 741]
- [45] B. Back, W. Bauer, and J. Harris, Proceedings of the 9th Winter Workshop on Nuclear Dynamics, Key West, Florida, USA, 30 January – 6 February 1993
- [46] A. V. Ignatyuk, G. A. Kudyaev, A. Junghans, M. de Jong, H.-G. Clerc, and K.-H. Schmidt, Nucl. Phys. A 593 (1995) 519
- [47] J. Töke and W. J. Swiatecki, Nucl. Phys. A 372 (1981) 113
- [48] W. Reisdorf and J. Töke, Z. Phys. A 302 (1981) 183
- [49] A. V. Ignatyuk, M. G. Itkis, V. N. Okolovich, G. N. Smirenkin, and A. S. Tishin, Yad. Fiz. 21 (1975) 1185 [Sov. J. Nucl. Phys. 21 (1975) 612]
- [50] W. D. Myers and W. J. Swiatecki, Ann. Phys. 84 (1974) 186
- [51] A. J. Sierk, Phys. Rev. C 33 (1986) 2039
- [52] K. X. Jing, L. Phair, L. G. Moretto, Th. Rubehn, L. Beaulieu, T. S. Fan, and G. J. Wozniak, Phys. Lett. B 518 (2001) 221
- [53] S. Chandrasekhar, Rev. Mod. Phys. 15 (1943) 1

-
- [54] D. J. Hofman, B. B. Back, and P. Paul, Phys. Rev. C. 51 (1995) 2597
- [55] V. A. Rubchenya, A. V. Kuznetsov, W. H. Trzaska, D. N. Vakhtin, A. A. Alexandrov, I. D. Alkhazov, J. Äystö, S. V. Khlebnikov, V. G. Lyapin, O. I. Osetrov, Yu. E. Penionzhkevich, Yu. V. Pyatkov, and G. P. Tiourin, Phys. Rev. C 58 (1998) 1587
- [56] J. Taïeb, Ph. D. Thesis, INP Orsay, France, (2000)
- [57] R. W. Hasse and W. D. Myers, “Geometrical Relationships of Macroscopic Nuclear Physics” Springer-Verlag Berlin Heidelberg 1988 ISBN 3-540-17510-5
- [58] W. D. Myers and W. Swiatecki, Nucl. Phys. 81 (1966) 1